Growth hormone receptor (GHR)-expressing neurons in the hypothalamic arcuate nucleus regulate glucose metabolism and energy homeostasis

Juliana Bezerra Medeiros de Lima, Lucas Kniess Debarba, Manal Khan, Chidera Ubah, Olesya Didyuk, Iven Ayyar, Madelynn Koch, and Marianna Sadagurski

Department of Biological Sciences, Integrative Biosciences Center (IBio), Wayne State University, Detroit, Michigan, MI

Corresponding author:
Marianna Sadagurski,
Department of Biological Sciences,
Integrative Biosciences Center
Wayne State University
Room 2418 IBio,
6135 Woodward, Detroit, MI 48202
Phone: (313) 577 8637
Email: sadagurski@wayne.edu

Competing Interests Statement: The authors declare no competing interests.

Abbreviations

CNS, central nervous system; GH, growth hormone; GHR, growth hormone receptor; STAT5, signal transducer and activator of transcription 5; POMC, proopiomelanocortin; ARC, arcuate nucleus of the hypothalamus; DMH, dorsomedial hypothalamic nucleus; LHA, lateral hypothalamus; PVH, paraventricular hypothalamic nucleus; SST, somatostatin; GHRH, growth hormone releasing hormone; AgRP, agouti-related peptide

Abstract

Growth hormone (GH) receptor (GHR), expressed in different brain regions, is known to participate in the regulation of whole-body energy homeostasis and glucose metabolism. However, GH activation of these GHR-expressing neurons is less studied. We have generated a novel GHR-driven Cre recombinase transgenic mouse line (GHR^{cre}) in combination with the floxed tdTomato reporter mouse line we tracked and activated GHR-expressing neurons in different regions of the brain. We focused on neurons of the hypothalamic arcuate nucleus (ARC) where GHR was shown to elicit a negative feedback loop that regulates GH production. We found that ARC^{GHR+} neurons are co-localized with AgRP, GHRH, and somatostatin neurons, which were activated by GH stimulation. Using designer receptors exclusively activated by designer drugs (DREADDs) to control GHR^{ARC} neuronal activity, we revealed that activation of GHR^{ARC} neurons was sufficient in regulating distinct aspects of energy balance and glucose metabolism. Overall, our study provides a novel mouse model to study *in vivo* regulation and physiological function of GHR-expressing neurons in various brain regions. Furthermore, we identified for the first time specific neuronal population that responds to GH and directly linked it to metabolic responses *in vivo*.

Introduction

A cumulative body of evidence established that growth hormone (GH) plays pivotal roles in the regulation of systemic metabolism, through activation of the GH receptor (GHR) in the liver, muscle, adipose, and other tissues (1-6). In the central nervous system (CNS), GH is present in regions known to participate in the regulation of feeding, energy balance, and glucose metabolism, including the hypothalamus, hippocampus, and amygdala (7-11). The expression of GHR within the CNS has been mapped by *in situ* hybridization and by detection of the downstream target, the phosphorylated activator of transcription (STAT) 5, revealing large numbers of GH-responsive neurons in various brain regions (8,12,13). While these studies detected GHR expression within the CNS, the functional assessment of the GHR-expressing neurons in various brain regions was lacking.

GHR expression in the brain is critical for the neuroendocrine neurons to sense and regulate GH production by the pituitary (8,14,15). In the arcuate nucleus of the hypothalamus (ARC), the GHR is involved in a negative feedback loop that regulates GH production and secretion by GH-releasing hormone (GHRH) (8). As part of this negative feedback, GH inhibits it's own secretion acting on the GHR in neuropeptide Y (NPY) neurons in the ARC and somatostatin (SST) neurons in the paraventricular nucleus (PVN). Activation of these neurons augments SST release and inhibits GH secretion (16,17). In recent years, it became clear that GH action in the ARC represents an important component of energy homeostasis (13). We have recently shown that neuronal-specific deletion of GHR in leptin receptor (LepRb)-expressing neurons in the hypothalamus impaired hepatic glucose production and systemic lipid metabolism (18). Additionally, mice lacking GHR specifically in the orexigenic agouti-related peptide (AgRP) expressing neurons in the ARC display impaired responses to fasting and food restriction, while deletion of GHR from anorexigenic proopiomelanocortin (POMC) neurons in the ARC did not produce significant metabolic phenotype (19,20). Collectively, these results indicated unique roles of GHR-expressing neurons in the ARC in metabolic control. However, in vivo GH-mediated activation of GHR-expressing neurons were not studied.

In the current study, we specifically aimed at studying in vivo activation of these complex neural circuitry of the GHR-expressing neurons in the ARC. To that end, we developed a novel GHR-

driven cre mouse (GHR^{cre}) using the CRISPR/Cas9 gene-editing technology. The new GHR^{cre} model allowed us to both track and activate GHR-expressing neurons. Utilizing these mice, we studied the functional roles of GHR neurons in the ARC in the regulation of systemic glucose metabolism and energy homeostasis. We found that activation of GHR^{ARC} neurons acutely increased systemic glucose sensitivity, energy expenditure, and heat production. Overall, our study revealed a novel network of metabolic regulation through the hypothalamic GH axis in the ARC. Finally, our mouse model provides a novel tool to identify specific neuronal populations mediating the effects of GH in different brain regions.

Materials and Methods

Experimental Animals:

GHR^{cre} mice were generated using the Clustered Regularly Interspaced Short Palindromic Repeats associated protein Cas9 (CRISPR/Cas9) technology (21,22). All procedures were performed at the University of Michigan Transgenic Core as before (22). A detailed description of the procedures is described in Supplementary Materials and Methods. tdTomato mice on the ROSA26 background (B6.Cg-Gt(ROSA)26Sort$^{m14(CAG-tdTomato)Hze}$/J, (stock 007914) were purchased from The Jackson Laboratory. Adult male mice (8-12 weeks old) were used for all studies. All mice were provided *ad libitum* access to standard chow diet (Purina Lab Diet 5001) and housed in temperature-controlled rooms on a 12-hour/12-hour light-dark cycle. Mice were bred and housed within our colony according to guidelines approved by the Wayne State University Committee on the Care and Use of Animals.

Perfusion and Histology:

Mice were anesthetized (IP) with avertin and transcardially perfused with phosphate-buffered saline (PBS) (pH 7.5) followed by 4% paraformaldehyde (PFA). Brains were post-fixed, sank in 30% sucrose, frozen in OCT medium, and then sectioned coronally (30 µm) and processed for immunohistochemistry as previously described (23,24). For immunohistochemistry, free-floating brain sections were washed in PBS, blocked using 3% normal donkey serum (NDS) and 0.3% Triton X-100 in PBS and then stained with a primary antibody for 48 hours at 4°C with agitation in blocking buffer: DsRed (anti-rabbit, 1:5000, cat. number NC9580775, Takara), GFP (anti-chicken, 1:1000, cat. number ab13970, Abcam), anti-tdTom (anti-goat, 1:500, cat. number AB8181-200, Scigen), pSTAT5 (anti-rabbit, 1:500, cat. number 9359, Cell Signaling), GFAP (anti-chicken, 1:500, cat. number Ab5541, Millipore), Iba-1 (anti-goat, 1:1000, cat. number ab5076, Abcam) and cFos (anti-sheep, 1:500, cat. number ab6167, Abcam) For pSTAT5 staining sections were pretreated for 10 min in 90% Methanol and 10% H_2O_2 in PBS before blocking buffer incubation. On the following day, all floating brain sections were washed with PBS 0.1M and incubated with the following secondary antibodies for

2 hours: donkey anti-rabbit, anti-goat, anti-sheep, anti-chicken Alexa Fluor 488 and/or 568 (Invitrogen, 1:200). For the staining specificity control, the immunohistochemical experiments were performed with brain sections in which the primary antibody was omitted and substituted with serum.

Two-plex fluorescent in-situ hybridization:

Fixed-frozen ARC-containing GHR^{cre} brain sections of 12-week old male mice (10µm) were processed for the RNAscope Fluorescent Multiplex assay (Advanced Cell Diagnostics, Inc). The samples were double-labeled with probes for GHR (Mm-Ghr-C2 464951), GHRH (Mm-Ghrh-C2 470991), or SST (Mm-Sst-C2 404631) together with tdTom (tdTomato-C3 317041).

Images and data analysis:

All sections used for ISH were visualized with a Zeiss M2 microscope blindly. All other fluorescent sections were visualized with a Nikon Eclipse Ni microscope coupled to a Nikon DS-Ri2 camera. Photomicrographs were captured using the NIS-Elements Br 5.0 Zen software. Fiji ImageJ image-editing software was used to overlay photomicrographs to construct merged images and to mount plates. Only sharpness, contrast, and brightness were adjusted and the same values for each target labeled were applied.

Surgery and viral injections:

Stereotaxic viral injections were performed as described (25). Briefly, animals were anesthetized using 1-3% isoflurane, their head shaved and placed in a three-dimensional stereotaxic frame (Kopf 1900, Cartesian Research Inc., CA). The skull was exposed with a small incision, and two small holes were drilled for bilateral microinjection (200 nL/side) of the excitatory DREADD, AAV8-hSyn-DIO-hM3DGq-mCherry (cat. number # 44361-AAV8, Addgene) into the ARC of GHR^{cre} mice at stereotaxic coordinates based on the Mouse Brain Atlas: A/P: -1.3, M/L: +/-0.2, D/V: -5.85 (26). Animals received a pre-operative dose of buprenorphine hydrochloride (1 mg/kg). After surgery, mice were allowed 2 weeks of recovery to maximize virally-transduced gene expression and to acclimate

168 animals to handling and experimental paradigms before the study. Activation of the DREADD receptor
169 was induced by intraperitoneal administration of the agonist, clozapine-N-oxide (CNO, 0.3 mg/kg, ip,
170 cat. number 4936, Tocris). Expression was verified post hoc in all animals, and any data from animals
171 in which the transgene expression was located outside the targeted area were excluded from analysis.
172
173 **Metabolic Analysis:**
174 Following recovery, GHR^{cre} mice with activating DREADD (hM3Dq) underwent glucose
175 metabolism and energy expenditure assays as previously described (27). Intraperitoneal glucose
176 tolerance tests were performed on mice fasted for 6 hours. Mice were administered with 0.9% saline
177 or CNO 1 hour before glucose (2 g/kg BW) injection. GTTs tests were performed one week apart and
178 blood glucose levels were measured as before (28). Blood insulin was determined using a Mouse
179 Insulin ELISA kit (cat. number 50-194-7920, Crystal Chem. Inc.). For peripheral GH stimulation
180 (recombinant mouse GH, 12.5 µg/100g BW, National Hormone & Peptide Program, Harbor-UCLA
181 Medical Center, CA), mice were injected i.p. and perfused 1.5 hours later, for pSTAT5 immunostaining
182 as described before (18). Metabolic measurements of energy homeostasis were obtained using an
183 indirect calorimetry system (PhenoMaster, TSE system, Bad Homburg, Germany). The mice were
184 acclimatized to the cages for 3 days and monitored for 5 days, food and water were provided *ad*
185 *libitum*. Following acclimatization, GHR^{cre} excitatory DREADD-expressing mice received an i.p.
186 injection of vehicle (0.9% saline) and measurements were analyzed for the following 8 hours. Mice
187 remained in the chambers with food and water *ad libitum* and 72 hours later the same experimental
188 design was repeated, and animals were treated with an i.p. injection of CNO (0.3 mg/kg). Data were
189 analyzed vehicle vs CNO per mouse.

190
191 **Statistical analysis:**

192 Unless otherwise stated mean values ± SEM is presented in graphics. GTT data were
193 analyzed by residual maximum likelihood (REML) mixed model followed by Sidak's post hoc while
194 cumulative RER, heat production, ambulatory activity, food intake, and water intake data were

195 analyzed through paired t-test. Post-hoc comparisons were only carried out when the p-value was

196 significant for effect and/or interactions. $p < 0.05$ was considered statistically significant.

197

Results

Characterization of the GHR^{cre} mice. To characterize the role of GHR-expressing neurons in the ARC, we have developed a GHR cell-specific molecular tool (GHR^{cre}) using CRISPR/Cas9 gene-editing technology (Supplementary Figure 1A). The GHR^{cre} mice reproduced in Mendelian ratio and both male and female mice exhibited normal body weight, and fed/fasting blood glucose levels (Supplementary Figure 1B and 2). GHR^{cre} mouse line was validated by a cre-dependent Rosa26-tdTomato reporter mouse. The expression pattern of tdTomato reporter revealed the presence of GHR^{cre}-expressing neurons in the several areas of the hypothalamus (Figure 1A), including the midbrain and hindbrain (Supplementary Figure 1C and Supplementary Table 1 and 2) (8,13). To validate the expression of GHR in our GHR^{tdTom} mice, we performed RNA *in situ* hybridization with RNAscope, using probes against *GHR* and *tdTomato* in the hypothalamic arcuate nucleus (ARC). As seen in Figure 1B, the majority of TdTomato^{+} neurons were positive for the expression of the *GHR* gene.

Upon binding to the GHR, GH triggers the activation of the JAK/Stat5 pathway (4,29,30). To track GH-mediated STAT5 phosphorylation (pSTAT5), acute intraperitoneal GH injection was given to the GHR^{tdTom} mice. We found that pStat5 was colocalized with the majority of the ARC^{GHR+} neurons (Figure 2A). We did not detect the colocalization of GHR^{tdTom+} cells in astrocytes positive to glial fibrillary acidic protein (GFAP). Additionally, the Iba1, a marker of microglia, did not co-localize with tdTomato (Figure 2B), indicating that GHR signaling is principally targeting neurons and not glia cells.

To determine whether GHR^{ARC+} neurons overlap with other known ARC populations that are involved in neuroendocrine regulation, we further examined the expression of *SST* and *GHRH* in identified GHR^{ARC+} neurons using double IHC and ISH. We found two-plex fluorescent ISH for *GHRH* or *SST* and *tdTomato* mRNAs colocalized in the ARC of GHR^{tdTom} mice (Figure 3), as previously reported (12). In support of previous studies (19,31), we further confirmed a substantial overlap of GHR^{+} neurons in the ARC with AgRP-expressing neurons in the GHR^{tdTom} mice (Supplementary Figure 3A). Additionally, in support of the single-cell sequencing data (31), we found a minimal

224 colocalization with dopaminergic neurons (GHR^{tdTom+}/TH^{+} cells), and with POMC neurons
225 (GHR^{tdTom+}/β-endorphin^{+} cells) in the ARC (Supplementary Figure 3B and 3C).
226

227 **GHR^{ARC+} neurons regulate glucose metabolism.** The hypothalamic GHR-expressing
228 neuronal circuits operate within complex physiological settings involving the interrelationships
229 between SST, GHRH, and AgRP-expressing neurons. We aimed to directly assess the contribution
230 of ARC GHR-expressing neuronal populations to glucose metabolism and energy homeostasis. To
231 achieve that, we employed a Cre-dependent DREADD (Designer Receptors Exclusively Activated by
232 Designer Drugs) virus to acutely modulate neuronal activity in response to peripheral injection of an
233 otherwise inert compound, clozapine N-oxide (CNO) (32-34). To determine whether activation of
234 GHR^{ARC+} neurons can influence blood glucose levels, we enhanced the GHR^{ARC+} neuronal activity of
235 GHR^{Cre} mice by stereotactically injecting AAV8-DIO-hM3Dq-mCherry into the ARC and activated the
236 transduced cells with CNO (Figure 4A). Specific activation of GHR^{ARC} neurons was demonstrated by
237 nuclear c-Fos expression as a marker of neuronal activation in AAV8-DIO-hM3Dq-mCherry-ARC-
238 injected GHR^{cre} mice treated with vehicle (data not shown) or CNO (Figure 4A) before perfusion. CNO
239 administration resulted in a significant increase in c-Fos expression in hM3Dq-expressing ARC
240 neurons. Basal blood glucose and serum insulin concentrations were indistinguishable between
241 baseline and CNO injected mice (Figure 4B and D). Each animal served as its own control (e.g.,
242 saline versus CNO). Despite unchanged fasting blood glucose levels, AAV8-DIO-hM3Dq-mCherry-
243 ARC CNO-treated GHR^{cre} mice displayed significantly increased glucose disposal, indicating
244 increased sensitivity in response to an intraperitoneal glucose load (AUC baseline: 1234 ± 88. 67 vs
245 AUC CNO: 1049 ± 84. 27, t-test $p < 0.05$, Figure 4B and C). Of note, the DREADD virus per se (off-
246 target infection, with or without CNO) did not affect glucose tolerance (data not shown).

247 **GHR^{ARC+} neurons regulate energy balance and heat production.** To establish the
248 significance of GHR^{ARC+} neurons in the control of energy utilization, we analyzed components of
249 energy expenditure in *ad libitum*-fed 12-week-old male GHR^{cre} mice. We injected mice with CNO in
250 the morning during the light cycle, a time in which mice normally refrain from eating. Using a single-

subject approach where each mouse serves as its own control, we showed that stimulation of GHR^{ARC+} neurons produced a significant increase in energy expenditure (Figure 5A), which lasted for approximately 8 hours. This effect was also associated with a significant increase in heat production in these CNO stimulated hM3Dq-ARC-injected GHR^{cre} mice (paired t-test, $p < 0.05$) (Figure 5B). CNO stimulated locomotor activity was equivalent to the baseline measurements (Figure 5C). Notably, acute activation of AgRP neurons markedly reduces energy expenditure (25), emphasizing the complexity of ARC GH-responsive neurons, and suggesting that $GHR^{ARC+}/AgRP^{-}$ neurons are critical to driving energy homeostasis.

Surprisingly, administering CNO to these mice acutely and significantly increased feeding and drinking responses (Figure 6A and B), suggesting that GHR^{ARC+} neurons are orexigenic neurons functionally similar to AgRP/SST neuronal cluster in the ARC (31).

Discussion

We present herein a novel mouse model that expresses cre recombinase driven by the GHR promoter. Specifically, using tdTomato immunoreactivity as a marker of GHR expression in GHR^{tdTom} mice, we unraveled the uncharacterized population of GHR expressing neurons in the ARC. Further, using a site-specificity approach we have characterized the function of GHR^{+} population in the ARC. Using a combination of a genetic mouse model with site-specific delivery of chemogenetic agent (CNO) we identified, for the first time, a GHR^{ARC+} neuronal population that plays a critical role in the maintenance of peripheral glucose metabolism and energy homeostasis.

The distribution of GHR-expressing neurons in the brain by GHR^{dTom} reporter resembles that determined by *in situ* hybridization and by systemic GH injections followed by pSTAT5 expression pattern in the brain (8,12,13). Large populations of GHR-expressing neurons lay in the hypothalamus, especially in the ARC, DMH, and VMH; other substantial populations reside in the posterior hypothalamic area and ventral pre-mammillary nucleus. The hippocampus areas, the cortex, the cerebellum, and the olfactory area also contain substantial concentrations of GHR-expressing neurons. The nucleus tractus solitarius (NTS) represents the hindbrain site with significant numbers of GHR-expressing neurons. Another substantial number of GHR- expressing neurons were distributed in the thalamus region. These observations are consistent with the expected expression pattern of GHR in the brain (8,12,13), and for the first time enabled us to study the function of specific GHR populations throughout the brain.

Evidence for the importance of GH-responsive neurons in the hypothalamus in modulating metabolism was reported in several studies (35-38). We have recently identified a unique population of nutrient-sensing leptin receptor (LepRb)-GHR expressing neurons that regulate hepatic glucose production and lipid metabolism, suggesting that these neurons are crucial for the metabolic functions of GHR-neurocircuitry (18). LepRb neurons co-express GHR in the ARC, DMH, and LHA, suggesting the role of GHR in these neurons as an integrating site of glucose metabolism regulation. In the ARC there is minimal overlap between AgRP neurons and SST neurons, with some transcriptional similarities between these neurons such as in their synaptic circuitry and function (31,39). Recent

single-cell analysis of ARC neurons demonstrated that GHR is highly expressed in the tight cluster of $AgRP^{+}/SST^{+}$ neurons together with corticotropin-releasing factor receptor 1 (*Crhr1)* (31), suggesting the potential role of these ARC neurons in GH neurocircuitry.

The circuitries engaged by GHR^{ARC} neurons involve several neuroendocrine populations such as the SST, GHRH, and AgRP since GHR^{ARC} neurons are co-localized with these cells in the ARC. The majority of GHR^{ARC+} neurons in the ARC are also pSTAT5 immunoreactive after GH treatment, confirming their sensitivity to GH. We showed that chemogenetic activation of GHR^{ARC+} neurons modulated both glucose metabolism and energy homeostasis indicating that GHR^{ARC+} neurons lie within energy balance and glucoregulatory neurocircuits. While our current studies do not indicate which specific neuronal subpopulations within GHR^{ARC} are responsible for controlling each of these distinct physiological responses, genetic deletion of GHR in AgRP neurons did not affect glucose metabolism or energy homeostasis (19), indicating that the role of GHR in $AgRP^{-}$ populations in the ARC is to coordinate these responses. GHR^{ARC} neurons only partially overlap with SST and GHRH neurons, thus the contribution of these ARC neuronal populations to GHR^{ARC}-mediated glucose metabolism and energy homeostasis modulation remains to be clarified.

One of the established effects of GH in the ARC - is inhibition of its own secretion, as part of an auto-feedback circuit, involving the interrelationships between SST, GHRH, and AgRP/NPY - expressing neurons through GHR (40). This might be particularly important as properly regulated neural circuits within the GH axis modulate GH release under fed and fasting states (41), while the imbalance between these networks might be part of multiple maladaptive endocrine changes responsible for metabolic alterations in obesity. Our chemogenetic studies indicate that the hypothalamic GHR axis in ARC promotes glucoregulatory responses by enhancing glucose tolerance, and suggest that GHR^{ARC} neurons represent a distinct neuronal population within the GH axis that play a crucial role in the regulation of glucose metabolism. This effect is complementary to the counter-regulatory enhancing effect of GH axis during hypoglycemia (42).

GHR^{ARC} neurons represent a heterogeneous population, which includes neurochemically-defined neurons that control specific physiologic functions. For example, acute chemogenetic

activation of AgRP neurons alters food intake and decreases energy expenditure (25). Additionally, activation of AgRP neurons acutely impairs systemic insulin sensitivity by inhibiting glucose uptake in brown adipose tissue (43). However, while the majority of GHR^{+} neurons in the ARC colocalize with AgRP neurons, *GHR* represents only a very small cluster within AgRP neuronal population (31); therefore, it remains possible that other GHR^{+} neuronal populations in the ARC contribute to GHR^{ARC}-mediated modulation of energy balance. In support, chemogenetic activation of ARC-SST neurons, or intracerebroventricular (i.c.v.) infusion of SST analog acutely and significantly increases feeding responses (31,44). Infusion of SST analog also increases energy expenditure, drinking behavior, and lowers glycemic values (44), similar to the chemogenetic activation of GHR^{ARC} neurons. These findings indicate some functional similarities between SST and GHR^{ARC} neurons whose activation is sufficient in driving feeding, glucoregulation, and energy balance.

In summary, we have generated the GHR^{tdTom} mouse model to characterize the anatomical localization of brain-wide GHR expression. Using the GHR^{tdTom} mouse model we demonstrate that GHR^{ARC} comprises a unique neuronal population capable of controlling energy balance and glucose metabolism. While the significance of this ARC subpopulation of GH-responsive neurons in the control of certain aspects of energy balance and glucose regulation remains to be elucidated, our study emphasizes the role of GH axis as an essential hypothalamic center in regulating metabolic functions and provides a resource for studying the biology and functionality of GH-responsive neuronal populations in the brain.

Author contributions

JBML, LKD, carried out the research and reviewed the manuscript. IA, OD, CU, MK, and, MK carried out the research. MS designed the study, analyzed the data, wrote the manuscript, and is responsible for the integrity of this work. All authors approved the final version of the manuscript.

Acknowledgments

The authors thank Mohammed Alysofi and Hawraa Alromdhan for their technical assistance. This study was supported by the American Diabetes Association grant #1-lB-IDF-063, by a Feasibility Grant from the Michigan Diabetes Research Center (P30DK020572) and WSU funds for MS.

Competing interests.

The authors declare no competing interests.

Data Availability

The datasets generated during and/or analyzed during the current study are available from the corresponding author on reasonable request.

References:

1. Iida K, Del Rincon JP, Kim DS, Itoh E, Nass R, Coschigano KT, Kopchick JJ, Thorner MO. Tissue-specific regulation of growth hormone (GH) receptor and insulin-like growth factor-I gene expression in the pituitary and liver of GH-deficient (lit/lit) mice and transgenic mice that overexpress bovine GH (bGH) or a bGH antagonist. *Endocrinology*. 2004;145(4):1564-1570.
2. Pennisi PA, Kopchick JJ, Thorgeirsson S, LeRoith D, Yakar S. Role of growth hormone (GH) in liver regeneration. *Endocrinology*. 2004;145(10):4748-4755.
3. Yakar S, Setser J, Zhao H, Stannard B, Haluzik M, Glatt V, Bouxsein ML, Kopchick JJ, LeRoith D. Inhibition of growth hormone action improves insulin sensitivity in liver IGF-1-deficient mice. *J Clin Invest*. 2004;113(1):96-105.
4. Kopchick JJ, List EO, Kelder B, Gosney ES, Berryman DE. Evaluation of growth hormone (GH) action in mice: discovery of GH receptor antagonists and clinical indications. *Mol Cell Endocrinol*. 2014;386(1-2):34-45.
5. Cordoba-Chacon J, Majumdar N, List EO, Diaz-Ruiz A, Frank SJ, Manzano A, Bartrons R, Puchowicz M, Kopchick JJ, Kineman RD. Growth Hormone Inhibits Hepatic De Novo Lipogenesis in Adult Mice. *Diabetes*. 2015;64(9):3093-3103.
6. Bartke A. New findings in gene knockout, mutant and transgenic mice. *Exp Gerontol*. 2008;43(1):11-14.
7. Hojvat S, Baker G, Kirsteins L, Lawrence AM. Growth hormone (GH) immunoreactivity in the rodent and primate CNS: distribution, characterization and presence posthypophysectomy. *Brain Res*. 1982;239(2):543-557.
8. Kastrup Y, Le Greves M, Nyberg F, Blomqvist A. Distribution of growth hormone receptor mRNA in the brain stem and spinal cord of the rat. *Neuroscience*. 2005;130(2):419-425.
9. Lobie PE, Garcia-Aragon J, Lincoln DT, Barnard R, Wilcox JN, Waters MJ. Localization and ontogeny of growth hormone receptor gene expression in the central nervous system. *Brain research Developmental brain research*. 1993;74(2):225-233.
10. Lai Z, Roos P, Zhai O, Olsson Y, Fholenhag K, Larsson C, Nyberg F. Age-related reduction of human growth hormone-binding sites in the human brain. *Brain Res*. 1993;621(2):260-266.
11. Furigo IC, Metzger M, Teixeira PD, Soares CR, Donato J, Jr. Distribution of growth hormone-responsive cells in the mouse brain. *Brain Struct Funct*. 2017;222(1):341-363.
12. Burton KA, Kabigting EB, Clifton DK, Steiner RA. Growth hormone receptor messenger ribonucleic acid distribution in the adult male rat brain and its colocalization in hypothalamic somatostatin neurons. *Endocrinology*. 1992;131(2):958-963.
13. Wasinski F, Frazao R, Donato J, Jr. Effects of growth hormone in the central nervous system. *Arch Endocrinol Metab*. 2019;63(6):549-556.
14. Argetsinger LS, Carter-Su C. Mechanism of Signaling by Growth Hormone Receptor. *Physiol Rev*. 1996;76(4):1089-1107.
15. E C, LM S, R S, RV C, FF C, C D. Interaction between leptin and neuropeptide Y on in vivo growth hormone secretion. *Neuroendocrinology*. 1998;68(3):187-191.
16. Minami S, Kamegai J, Sugihara H, Suzuki N, Wakabayashi I. Growth hormone inhibits its own secretion by acting on the hypothalamus through its receptors on neuropeptide Y neurons in the arcuate nucleus and somatostatin neurons in the periventricular nucleus. *Endocr J*. 1998;45 Suppl:S19-26.

17. Chan YY, Steiner RA, Clifton DK. Regulation of hypothalamic neuropeptide-Y neurons by growth hormone in the rat. *Endocrinology*. 1996;137(4):1319-1325.
18. Cady G, Landeryou T, Garratt M, Kopchick JJ, Qi N, Garcia-Galiano D, Elias CF, Myers MG, Jr., Miller RA, Sandoval DA, Sadagurski M. Hypothalamic growth hormone receptor (GHR) controls hepatic glucose production in nutrient-sensing leptin receptor (LepRb) expressing neurons. *Mol Metab*. 2017;6(5):393-405.
19. Furigo IC, Teixeira PDS, de Souza GO, Couto GCL, Romero GG, Perello M, Frazao R, Elias LL, Metzger M, List EO, Kopchick JJ, J D, Jr. Growth hormone regulates neuroendocrine responses to weight loss via AgRP neurons. *Nat Commun*. 2019;10(1):662.
20. Quaresma PGF, Teixeira PDS, Furigo IC, Wasinski F, Couto GC, Frazao R, List EO, Kopchick JJ, Donato J, Jr. Growth hormone/STAT5 signaling in proopiomelanocortin neurons regulates glucoprivic hyperphagia. *Mol Cell Endocrinol*. 2019;498:110574.
21. Yamanaka Y. CRISPR/Cas9 Genome Editing as a Strategy to Study the Tumor Microenvironment in Transgenic Mice. *Methods Mol Biol*. 2016;1458:261-271.
22. Burger LL, Vanacker C, Phumsatitpong C, Wagenmaker ER, Wang L, Olson DP, Moenter SM. Identification of Genes Enriched in GnRH Neurons by Translating Ribosome Affinity Purification and RNAseq in Mice. *Endocrinology*. 2018;159(4):1922-1940.
23. Patterson CM, Bouret SG, Park S, Irani BG, Dunn-Meynell AA, Levin BE. Large litter rearing enhances leptin sensitivity and protects selectively bred diet-induced obese rats from becoming obese. *Endocrinology*. 2010;151(9):4270-4279.
24. Sadagurski M, Landeryou T, Cady G, Kopchick JJ, List EO, Berryman DE, Bartke A, Miller RA. Growth hormone modulates hypothalamic inflammation in long-lived pituitary dwarf mice. *Aging Cell*. 2015;14(6):1045-1054.
25. Krashes MJ, Koda S, Ye C, Rogan SC, Adams AC, Cusher DS, Maratos-Flier E, Roth BL, Lowell BB. Rapid, reversible activation of AgRP neurons drives feeding behavior in mice. *J Clin Invest*. 2011.
26. Gf P, Franklin K. The Mouse Brain In Stereotaxic Coordinates. Vol 1.
27. Sutton AK, Gonzalez IE, Sadagurski M, Rajala M, Lu C, Allison MB, Adams JM, Myers MG, White MF, Olson DP. Paraventricular, subparaventricular and periventricular hypothalamic IRS4-expressing neurons are required for normal energy balance. *Sci Rep*. 2020;10(1):5546.
28. Debarba LK, Mulka A, Lima JBM, Didyuk O, Fakhoury P, Koshko L, Awada AA, Zhang K, Klueh U, Sadagurski M. Acarbose protects from central and peripheral metabolic imbalance induced by benzene exposure. *Brain Behav Immun*. 2020.
29. Argetsinger LS, Carter-Su C. Growth hormone signaling mechanisms: Involvement of the tyrosine kinase JAK2. *Horm Res*. 1996;45(Supp.1):22-24.
30. Moutoussamy S, Kelly PA, Finidori J. Growth-hormone-receptor and cytokine-receptor-family signaling. *Eur J Biochem*. 1998;255(1):1-11.
31. Campbell JN, Macosko EZ, Fenselau H, Pers TH, Lyubetskaya A, Tenen D, Goldman M, Verstegen AM, Resch JM, McCarroll SA, Rosen ED, Lowell BB, Tsai LT. A molecular census of arcuate hypothalamus and median eminence cell types. *Nat Neurosci*. 2017;20(3):484-496.
32. Krashes MJ, Koda S, Ye C, Rogan SC, Adams AC, Cusher DS, Maratos-Flier E, Roth BL, Lowell BB. Rapid, reversible activation of AgRP neurons drives feeding behavior in mice. *J Clin Invest*. 2011;121(4):1424-1428.
33. Armbruster BN, Li X, Pausch MH, Herlitze S, Roth BL. Evolving the lock to fit the key to create a family of G protein-coupled receptors potently activated by an inert ligand. *Proc Natl Acad Sci U S A*. 2007;104(12):5163-5168.

34. Sternson SM, Atasoy D, Betley JN, Henry FE, Xu S. An Emerging Technology Framework for the Neurobiology of Appetite. *Cell Metab*. 2016;23(2):234-253.
35. Wasinski F, Furigo IC, Teixeira PDS, Ramos-Lobo AM, Peroni CN, Bartolini P, List EO, Kopchick JJ, Donato J, Jr. Growth Hormone Receptor Deletion Reduces the Density of Axonal Projections from Hypothalamic Arcuate Nucleus Neurons. *Neuroscience*. 2020;434:136-147.
36. Furigo IC, de Souza GO, Teixeira PDS, Guadagnini D, Frazao R, List EO, Kopchick JJ, Prada PO, Donato J, Jr. Growth hormone enhances the recovery of hypoglycemia via ventromedial hypothalamic neurons. *FASEB J*. 2019:fj201901315R.
37. Wasinski F, Pedroso JAB, Dos Santos WO, Furigo IC, Garcia-Galiano D, Elias CF, List EO, Kopchick JJ, Szawka RE, Donato J, Jr. Tyrosine Hydroxylase Neurons Regulate Growth Hormone Secretion via Short-Loop Negative Feedback. *J Neurosci*. 2020;40(22):4309-4322.
38. Irani BG, Donato J, Jr., Olson DP, Lowell BB, Sacktor TC, Reyland ME, Tolson KP, Zinn AR, Ueta Y, Sakata I, Zigman JM, Elias CF, Clegg DJ. Distribution and neurochemical characterization of protein kinase C-theta and -delta in the rodent hypothalamus. *Neuroscience*. 2010;170(4):1065-1079.
39. Everitt BJ, Meister B, Hokfelt T, Melander T, Terenius L, Rokaeus A, Theodorsson-Norheim E, Dockray G, Edwardson J, Cuello C, et al. The hypothalamic arcuate nucleus-median eminence complex: immunohistochemistry of transmitters, peptides and DARPP-32 with special reference to coexistence in dopamine neurons. *Brain Res*. 1986;396(2):97-155.
40. Bluet-Pajot MT, Tolle V, Zizzari P, Robert C, Hammond C, Mitchell V, Beauvillain JC, Viollet C, Epelbaum J, Kordon C. Growth hormone secretagogues and hypothalamic networks. *Endocrine*. 2001;14(1):1-8.
41. Fazeli PK, Klibanski A. Determinants of GH resistance in malnutrition. *J Endocrinol*. 2014;220(3):R57-65.
42. Tesfaye N, Seaquist ER. Neuroendocrine responses to hypoglycemia. *Ann N Y Acad Sci*. 2010;1212:12-28.
43. Steculorum SM, Ruud J, Karakasilioti I, Backes H, Engstrom Ruud L, Timper K, Hess ME, Tsaousidou E, Mauer J, Vogt MC, Paeger L, Bremser S, Klein AC, Morgan DA, Frommolt P, Brinkkotter PT, Hammerschmidt P, Benzing T, Rahmouni K, Wunderlich FT, Kloppenburg P, Bruning JC. AgRP Neurons Control Systemic Insulin Sensitivity via Myostatin Expression in Brown Adipose Tissue. *Cell*. 2016;165(1):125-138.
44. Stengel A, Coskun T, Goebel M, Wang L, Craft L, Alsina-Fernandez J, Rivier J, Tache Y. Central injection of the stable somatostatin analog ODT8-SST induces a somatostatin2 receptor-mediated orexigenic effect: role of neuropeptide Y and opioid signaling pathways in rats. *Endocrinology*. 2010;151(9):4224-4235.

Figure Legends:

Figure 1. GHR-expressing neurons in the hypothalamus. To visualize cre-expressing neurons, mice were crossed with tdTomato reporter mice. (A) Immunofluorescent image of GHR^{+} neurons in the hypothalamus (red, TdTomato). The dashed box indicates a region of the arcuate nucleus of the hypothalamus (ARC) that is digitally enlarged and shown as an inset. (B) Two-plex fluorescent *in situ* hybridization of *GHR* mRNA (green) and *tdTomato* mRNA (red) was performed on coronal slices in the ARC. The dashed box indicates the region of the ARC that is digitally enlarged and shown as inset demonstrating the colocalization of *GHR* and *tdTomato* mRNA (white arrows). 3V = Third ventricle. Scale bar: 100 µm.

Figure 2. Characterization of GHR-expressing neurons in the ARC. (A) GH signaling in GHR-expressing neurons in the ARC. Immunofluorescence for pSTAT5 in 12-week-old GHR^{tdTom} mice injected IP with vehicle (saline) or GH (12.5µg/100g BW; 1.5 hr). Representative images from the ARC of GHR^{tdTom} mice are shown. pSTAT5 (green), TdTomato (red), and merged images of the indicated mice (colocalization is shown by arrows). (B) Representative images of astrocytes identified by immunofluorescent detection of GFAP protein (green, upper panel) and microglia evaluated by Iba1 immunostaining (green, lower panel) in the ARC obtained from GHR^{tdTom} mice (red, TdTomato). 3V = Third ventricle. Scale bar: 100 µm.

Figure 3. GHR-expressing neurons colocalization with SST and GHRH in the ARC. Two-plex fluorescent *in situ* hybridization of (A) *SST* mRNA (green), *tdTomato* mRNA (red) and *DAPI* (blue), and (B) *GHRH* mRNA (green), *tdTomato* mRNA (red) and *DAPI* (blue) was performed on coronal slices containing the ARC. Dashed box indicates the region of the ARC that is digitally enlarged and shown as inset demonstrating the colocalization of *SST* and *tdTomato* mRNA or *GHRH* and *tdTomato*. 3V = Third ventricle. Scale bar: 100 µm.

Figure 4. Acute activation of GHR^{ARC} neurons increases glucose tolerance. (A) Neuronal activation by cFos (green) was assessed 90 minutes after CNO stimulation. IHC for mCherry (red) identifies AAV-hM3Dq expression in GHR^{ARC} neurons in the ARC. Merged image (green/red) and dashed box indicate the region of the ARC that is digitally enlarged and shown as inset demonstrating

the colocalization of cFos and mCherry. 3V =Third ventricle. Scale bar: 100 µm. (B) Glucose tolerance tests (GTT) of 12-week old male mice performed one week apart. Saline (0.1 mL/10 g BW – Baseline) or CNO (0.3 mg/kg BW i.p) was injected 1 hour before i.p. GTT. The effect of GHR^{ARC} activation was analyzed by residual maximum likelihood (REML) mixed model followed by Sidak's post hoc. (C) GTT area under the curve (AUC) was analyzed by a paired t-test. (D) Fasted insulin levels. Results are presented as mean ± SEM, n=7; * $p < 0.05$ compared to vehicle values

Figure 5. Acute activation of GHR^{ARC} neurons increases energy homeostasis but not ambulatory activity. (A) Respiratory exchange ratio (RER). (B) Heat production. (C) Ambulatory activity assessed by a total of beam breaks. Mice were acclimated in metabolic cages and i.p. injected with either saline (grey) or CNO (red) at 10:30 am. On the right side, AUC of the light cycle period from the treatment time. Data are from male mice, analyzed by paired t-test (mean ± SEM, n = 7; * $p < 0.05$ compared to vehicle values)

Figure 6. Acute activation of GHR^{ARC} neurons increases food and water intake. (A) Food intake. (B) Water intake. Mice were acclimated in metabolic cages and i.p. injected with either saline (grey) or CNO (red) at 10:30 am. Results are presented as mean ± SEM (filled area). On the right side, AUC of the light cycle period from the treatment time. Data are from male mice, analyzed by paired t-test (mean ± SEM, n = 7; * $p < 0.05$ compared to vehicle values

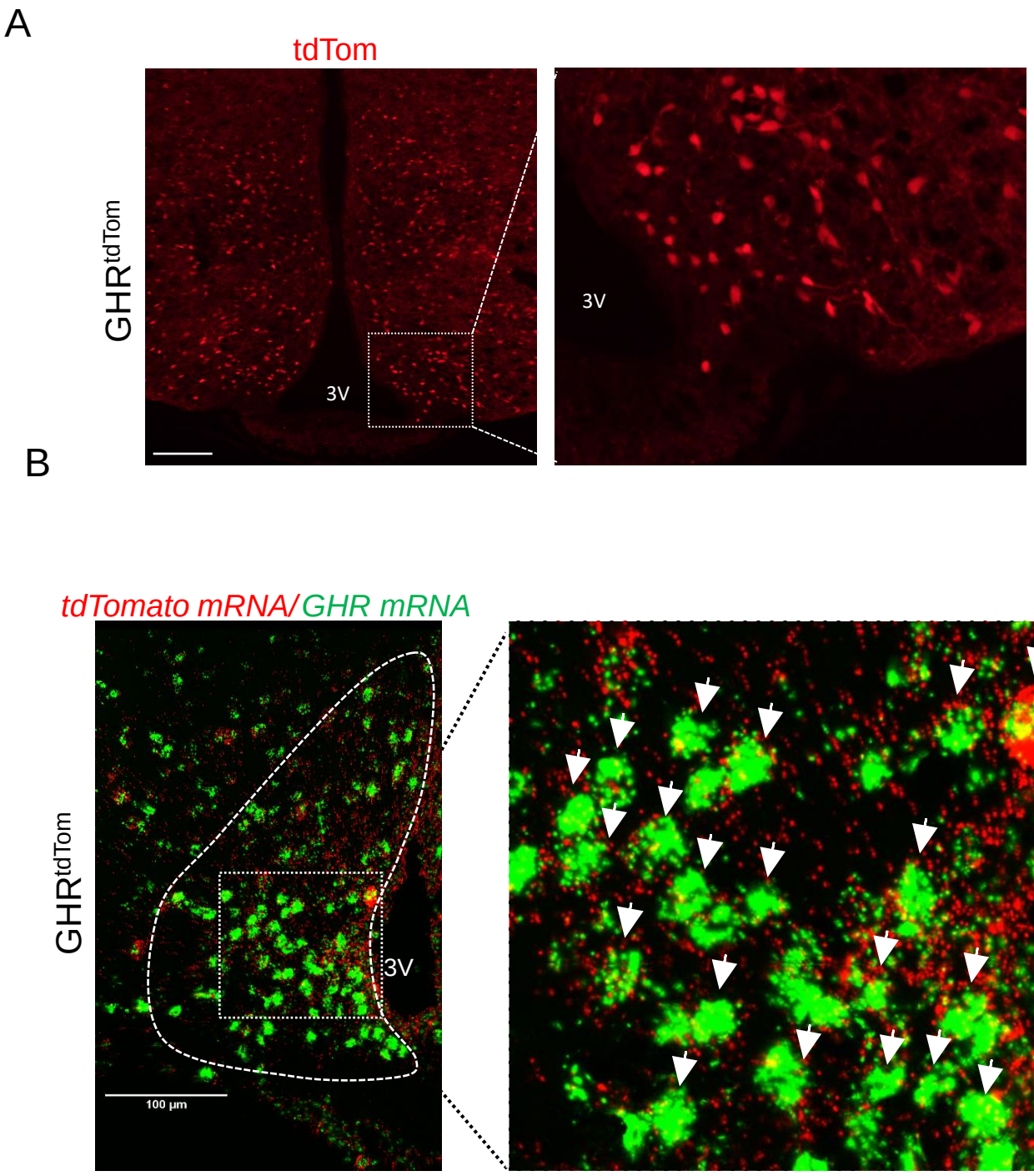
A
tdTom
GHRtdTom
3V
3V
B
tdTomato mRNA/GHR mRNA
GHRtdTom
3V
100 µm

Figure 1

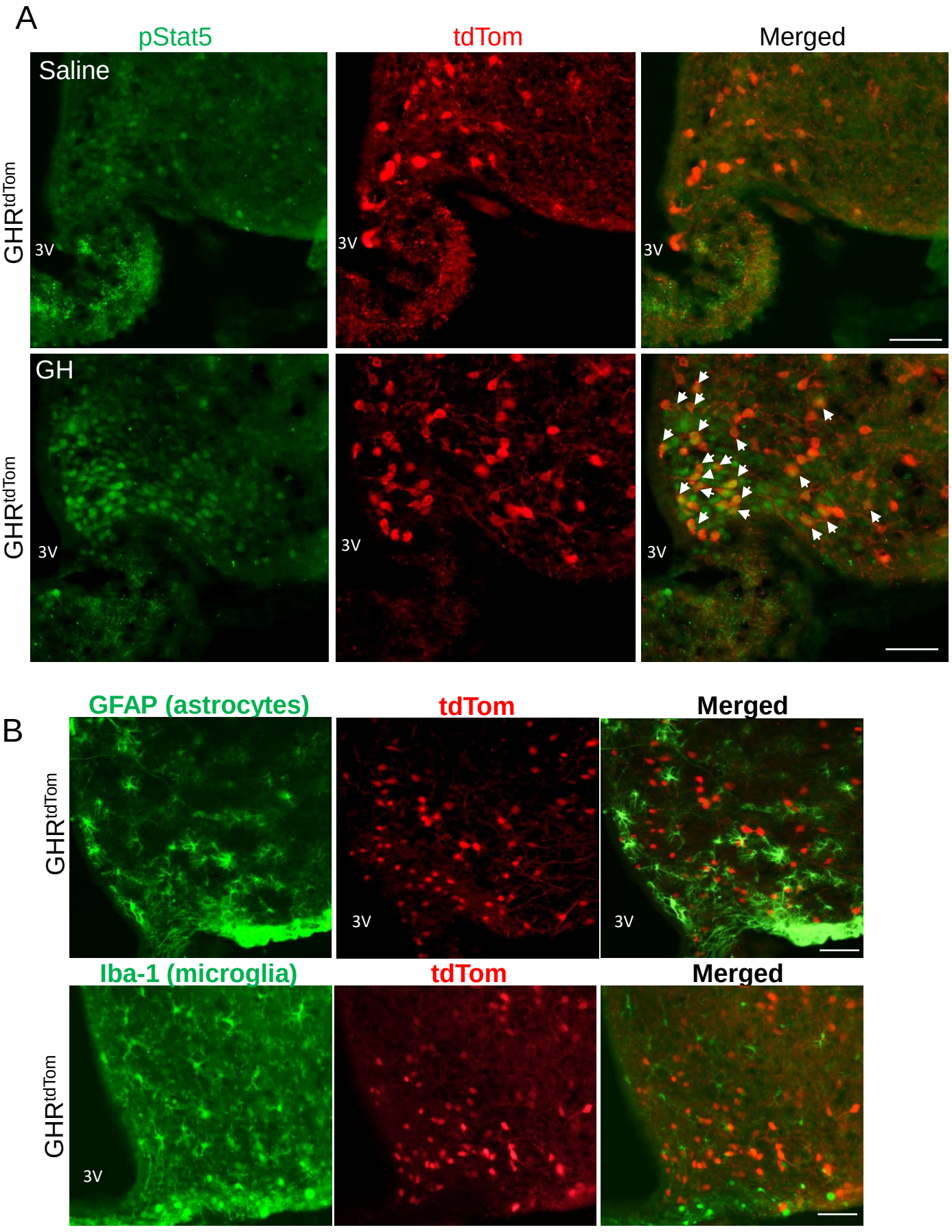
A
pStat5
tdTom
Merged
Saline
GHRtdTom
3V
GH
B
GFAP (astrocytes)
Iba-1 (microglia)

Figure 2

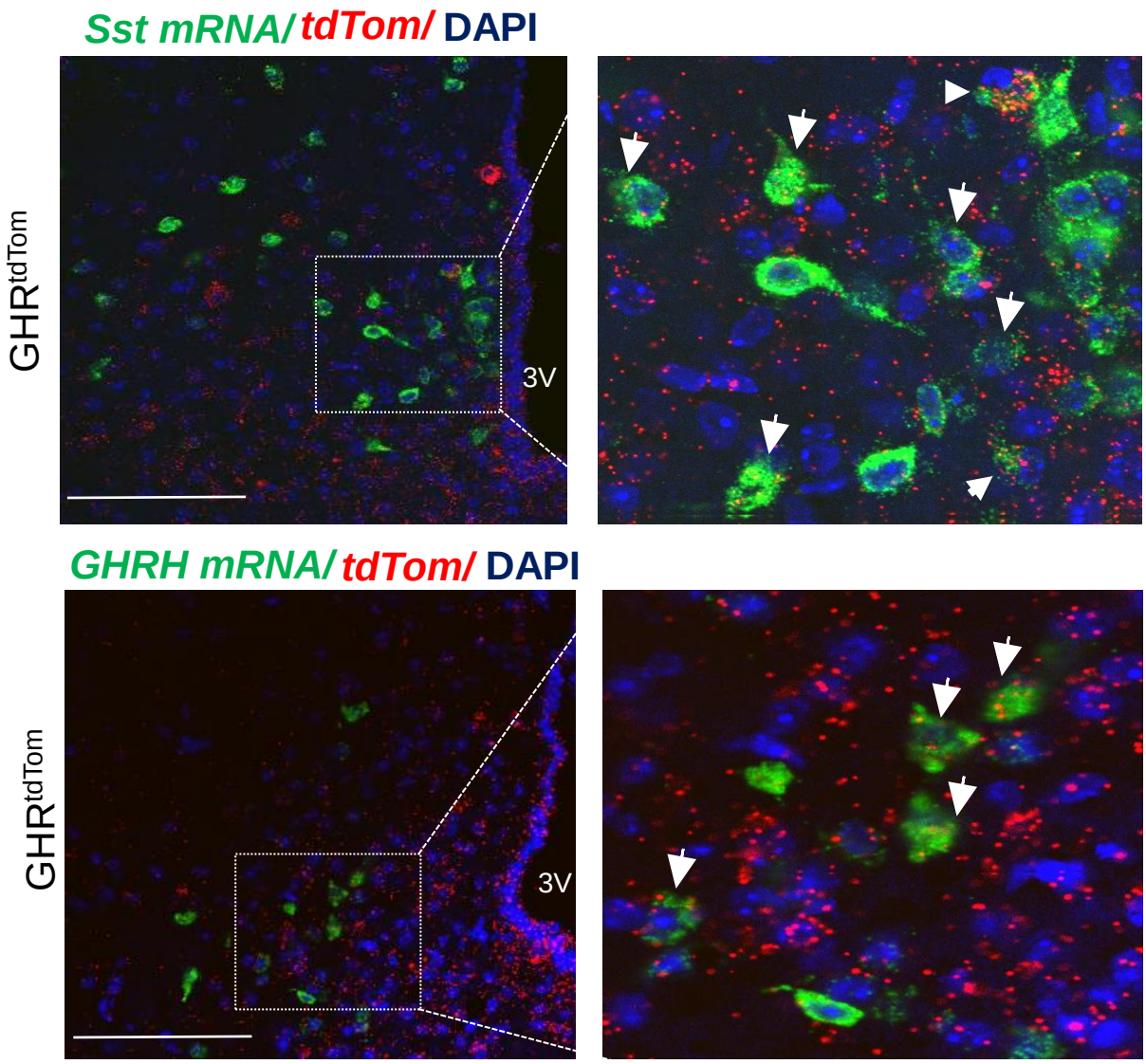
Sst mRNA/ tdTom/ DAPI
GHRtdTom
3V
GHRH mRNA/ tdTom/ DAPI
GHRtdTom
3V

Figure 3

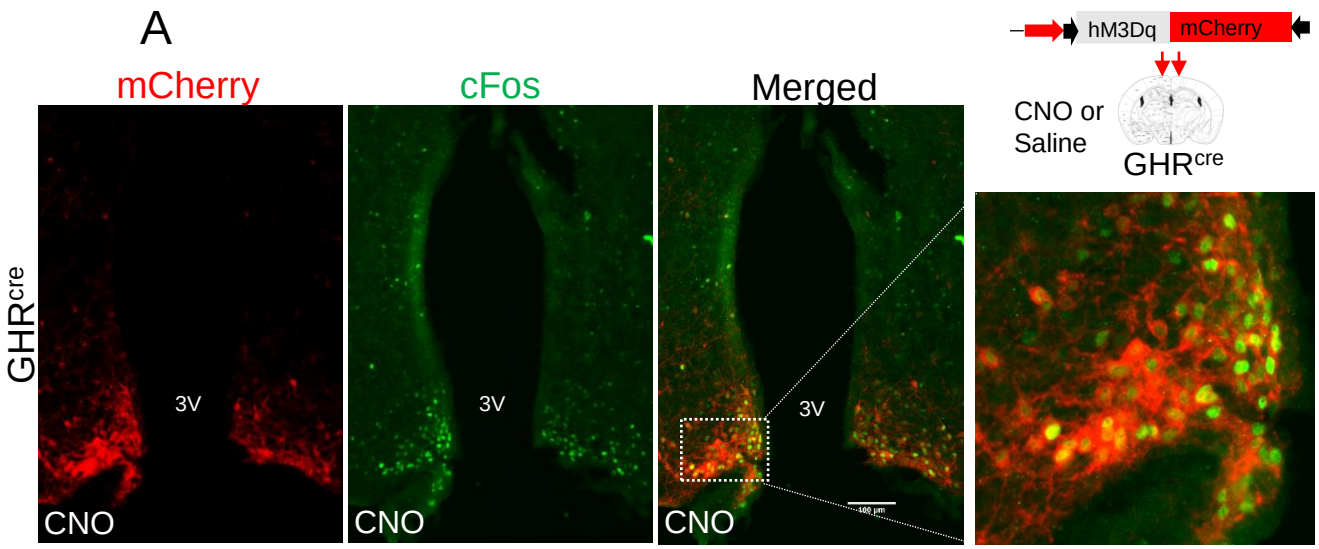
A
mCherry
cFos
Merged
GHRcre
3V
3V
3V
CNO
CNO
CNO
hM3Dq
mCherry
CNO or
Saline
GHRcre

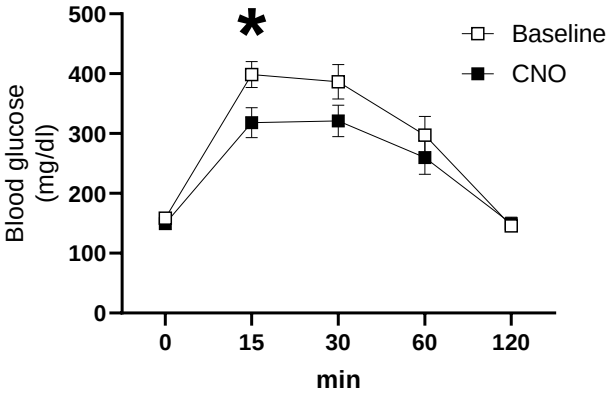
B
Blood glucose
(mg/dl)
500
400
300
200
100
0
*
Baseline
CNO
0
15
30
60
120
min

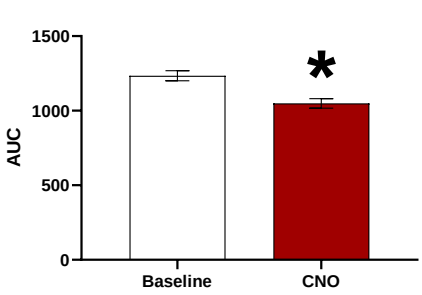
C
AUC
1500
1000
500
0
*
Baseline
CNO

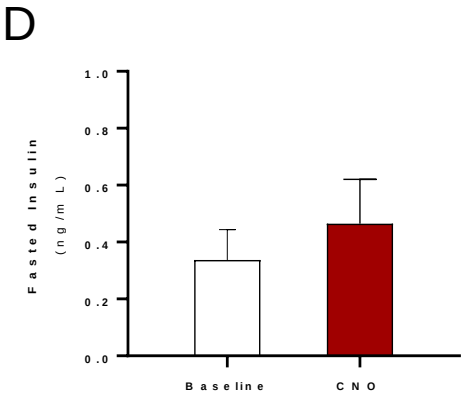
D
Fasted Insulin
(ng/mL)
1.0
0.8
0.6
0.4
0.2
0.0
Baseline
CNO

Figure 4

A

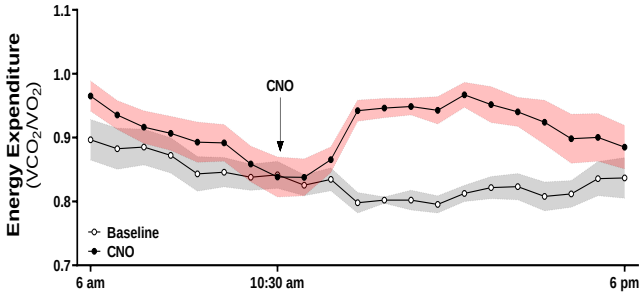
Energy Expenditure
(VCO2/VO2)
1.1
1.0
0.9
0.8
0.7
CNO
Baseline
CNO
6 am
10:30 am
6 pm

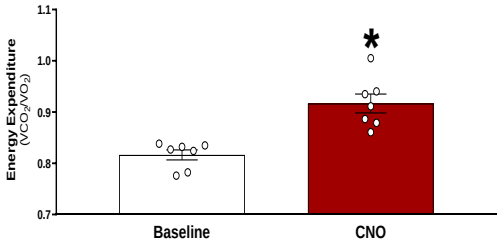
Energy Expenditure
(VCO2/VO2)
1.1
1.0
0.9
0.8
0.7
*
Baseline
CNO

B

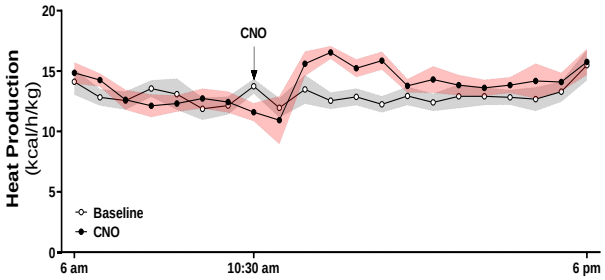
Heat Production
(kcal/h/kg)
20
15
10
5
0
CNO
Baseline
CNO
6 am
10:30 am
6 pm

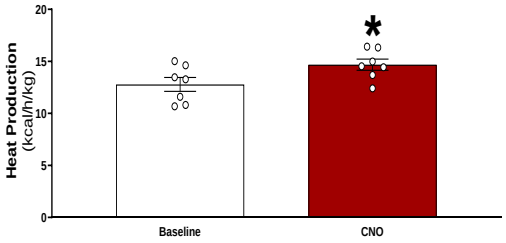
Heat Production
(kcal/h/kg)
20
15
10
5
0
*
Baseline
CNO

C

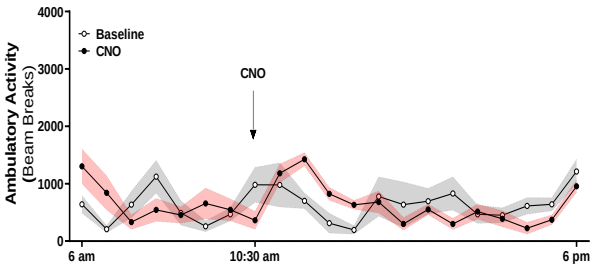
Ambulatory Activity
(Beam Breaks)
4000
3000
2000
1000
0
Baseline
CNO
CNO
6 am
10:30 am
6 pm

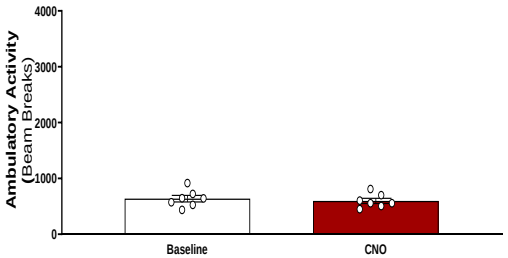
Ambulatory Activity
(Beam Breaks)
4000
3000
2000
1000
0
Baseline
CNO

Figure 5

A

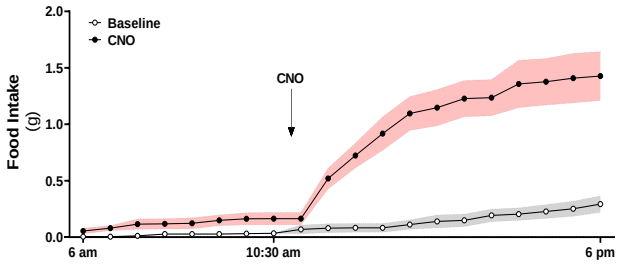
Baseline
CNO
CNO
Food Intake (g)
2.0
1.5
1.0
0.5
0.0
6 am
10:30 am
6 pm

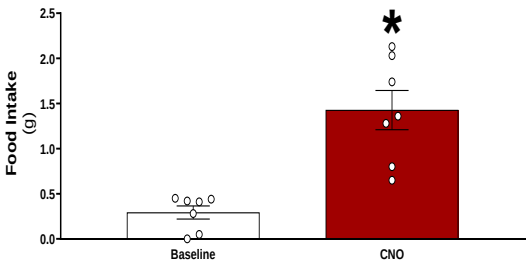
Food Intake (g)
2.5
2.0
1.5
1.0
0.5
0.0
*
Baseline
CNO

B

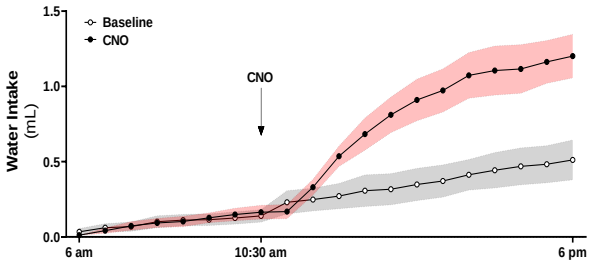
Baseline
CNO
CNO
Water Intake (mL)
1.5
1.0
0.5
0.0
6 am
10:30 am
6 pm

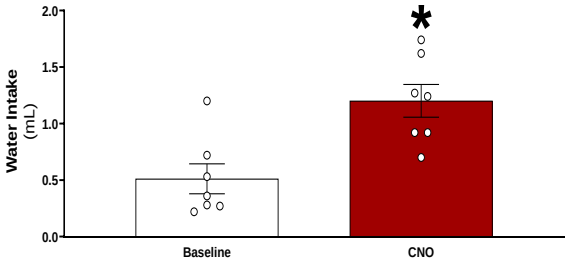
Water Intake (mL)
2.0
1.5
1.0
0.5
0.0
*
Baseline
CNO

Figure 6

SUPPLEMENTARY FIGURE 1

A

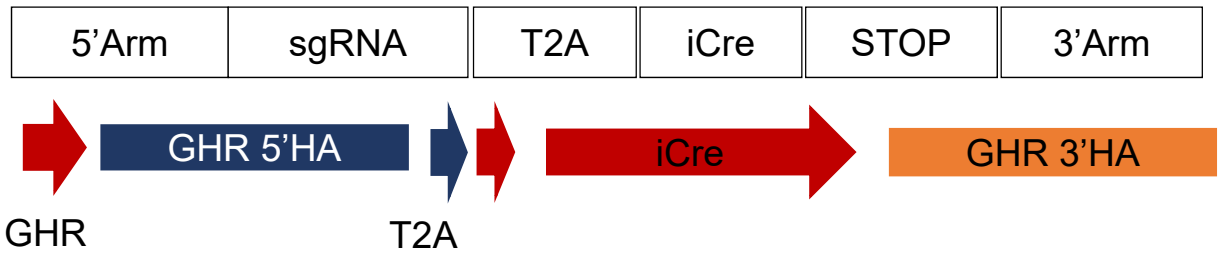

B

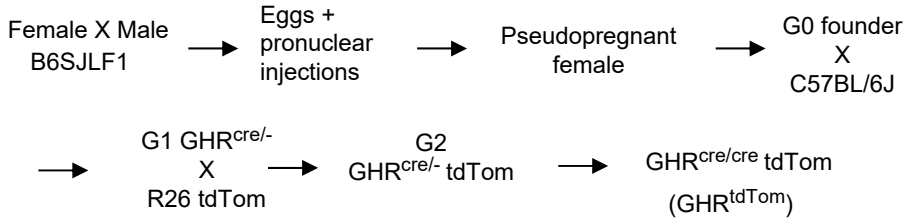

C

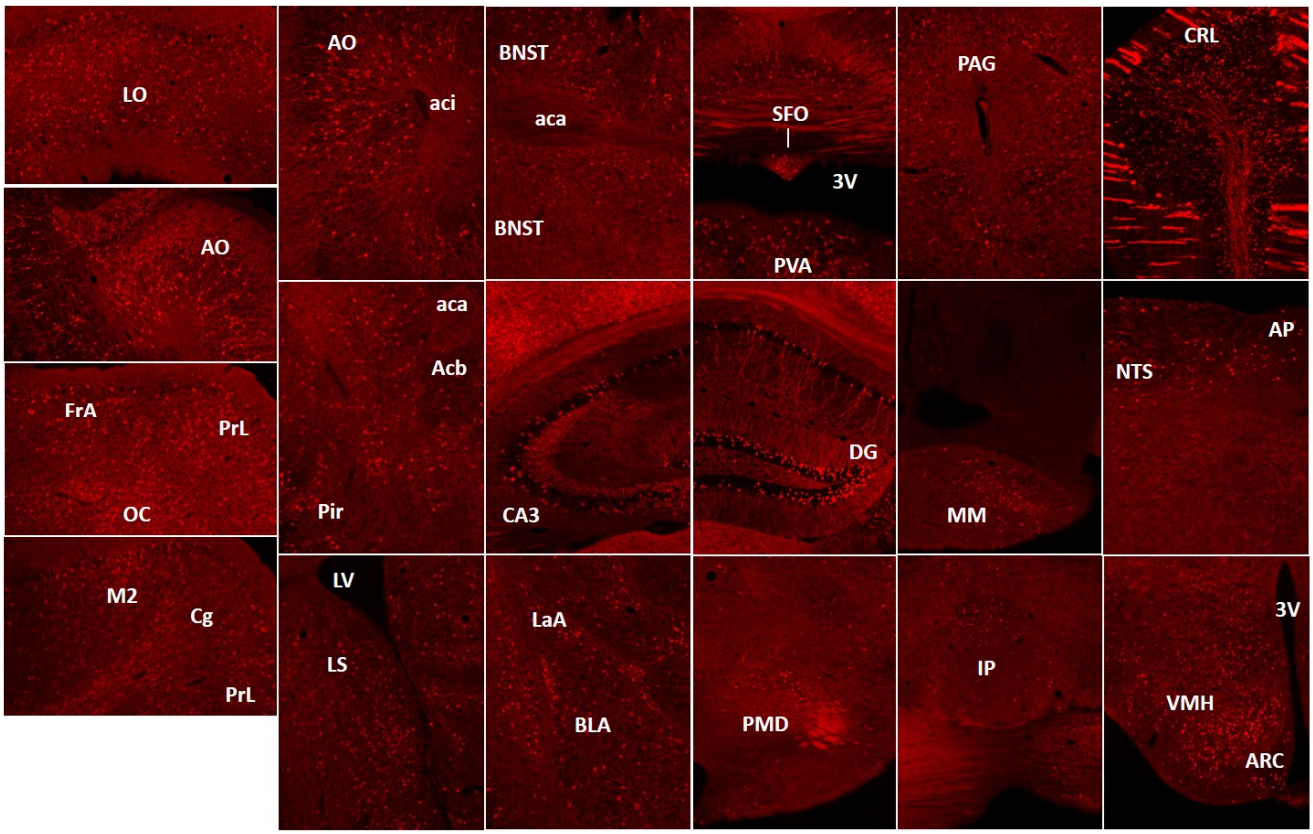

SUPPLEMENTARY FIGURE 2

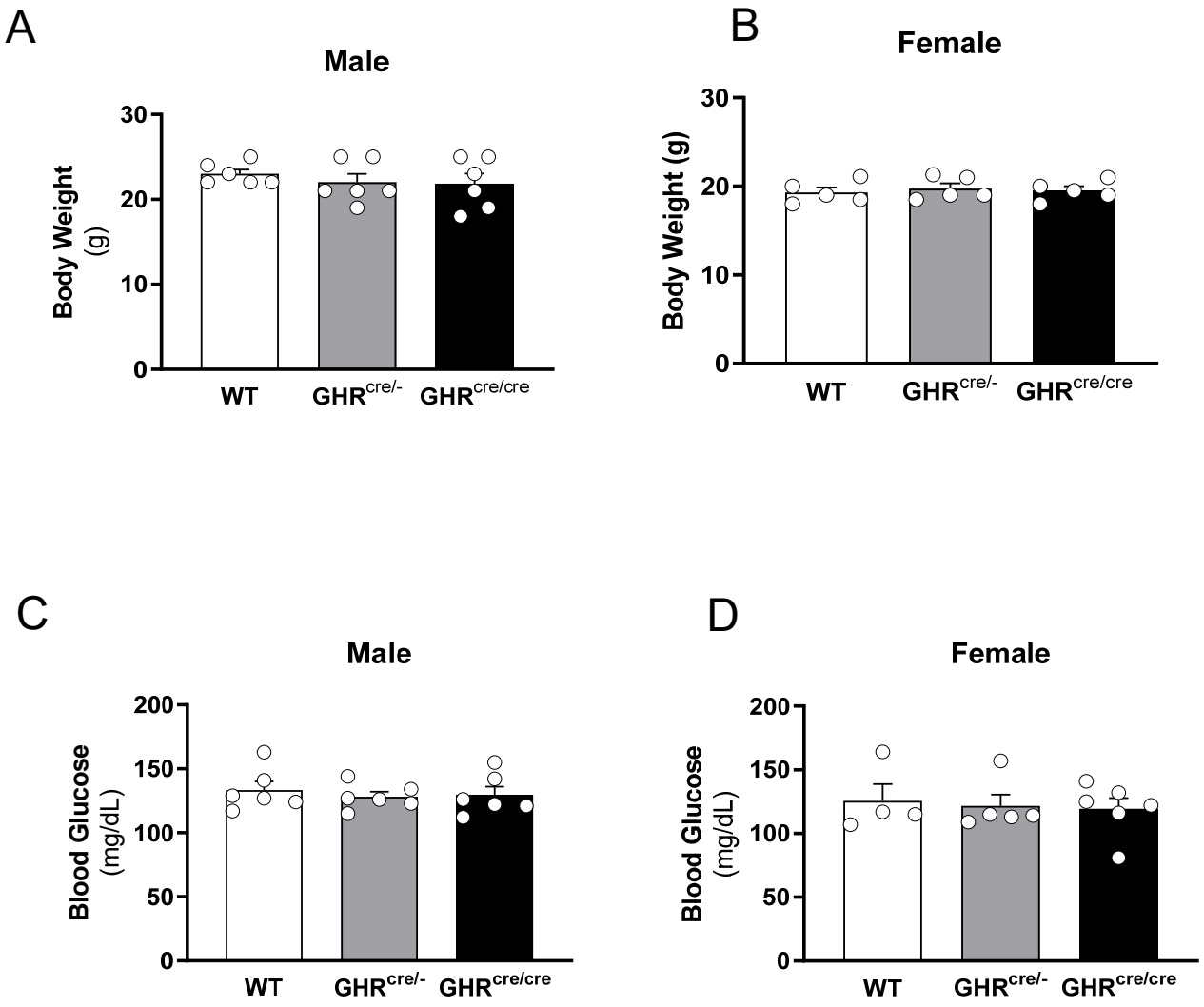

SUPPLEMENTARY FIGURE 3

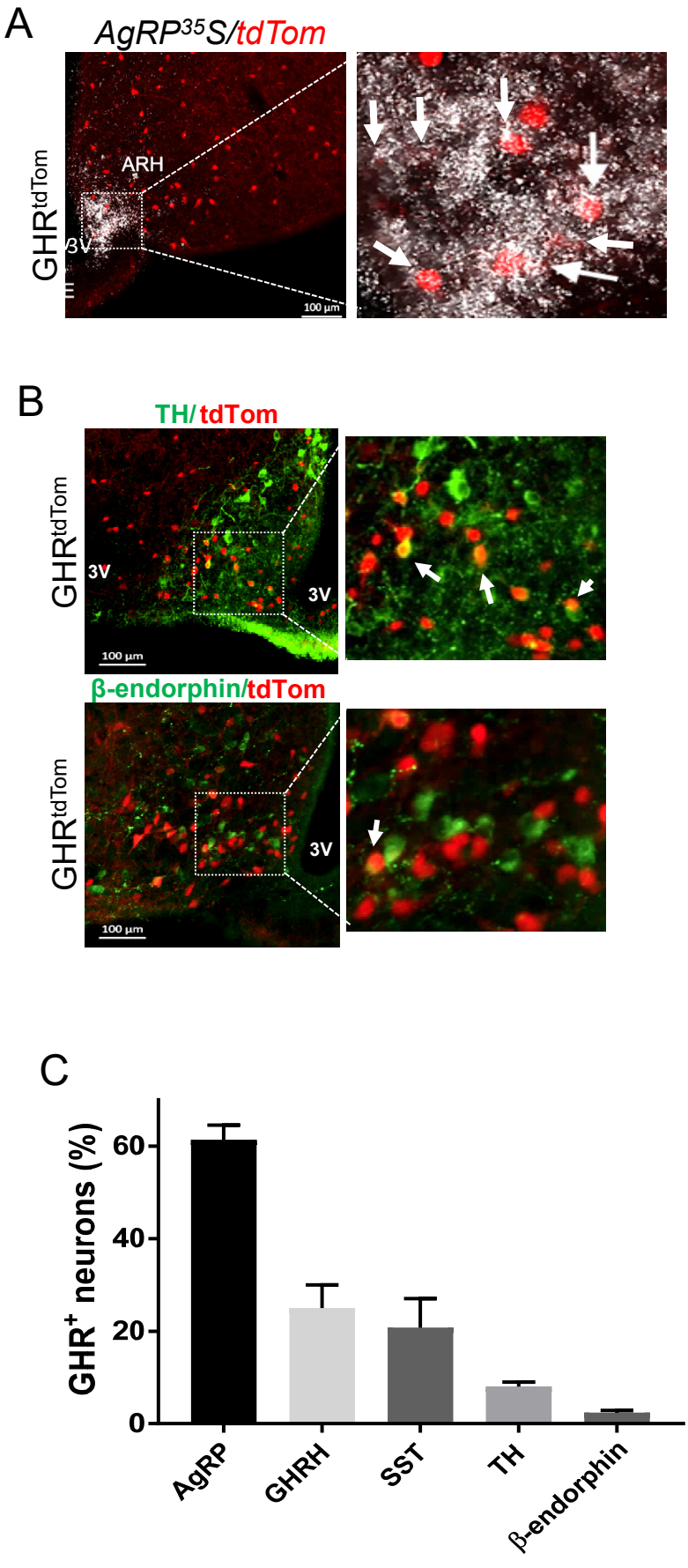

Distribution of $GHR^{cre/cre}$ TDTom immunoreactive neurons

	Brain areas and nuclei	$GHR^{cre/cre}$ tdTom-ir
LO	Lateral orbital cortex	++++
AO	Anterior olfactory area	++++
OC	Orbital cortex	++
PrL	Prelimbic cortex	+++
M2	Secondary motor cortex	++
Cg	Cingulate cortex	++
Pir	Piriform cortex	++
Acb	Accumbens nucleus	++
LS	Lateral septal nucleus	+++
BNST	Bed nucleus of the stria terminalis	++
SFO	Subfornical organ	++++
PVA	Paraventricular thalamic nucleus	+++
DG	Dentate gyrus	+++
CA3	Field CA3 hippocampus	++
LaA	Lateral amygdala	++
BLA	Basolateral amygdala	++
PMd	Dorsal premammillary nucleus	+
PAG	Periaqueductal gray	++
MM	Mammillary nucleus	++
IP	Interpeduncular nucleus	+
CRL	Cerebellum	++++
NTS	Nucleus of solitary tract	++
AP	Area postrema	++

Table 1

Distribution of $GHR^{cre/cre}$ TDTom immunoreactive neurons

	hypothalamic areas and nuclei	$GHR^{cre/cre}$ tdTom-ir
MPOa	Medial preoptic area	+
RCH	Retrochiasmatic area	++
PVH	Paraventricular nucleus	++
ARH	Arcuate nucleus	++
VMH	Ventromedial nucleus	+++
DMh	Dorsomedial nucleus	+++
LHA	Lateral hypothalamic area	+
DA	Dorsal hypothalamic area	+
pHA	Posterior hypothalamic area	+++
pmV	Ventral premammillary nucleus	++

Table 2